

The Dynamical Roche Lobe in Hierarchical Triples

Rosanne DiStefano,^{1*}

¹*Harvard-Smithsonian Center for Astrophysics, 60 Garden St., Cambridge MA 02138, US*

29 March 2019

ABSTRACT

The Roche lobe formalism describes mass transfer from one star to another. We develop an extension to hierarchical triples, considering the case in which a star donates mass to a companion which is itself a binary. The L1 point moves as the inner binary rotates, and the Roche lobe pulsates with the period of the inner binary. Signatures of mass transfer may therefore be imprinted with the orbital period of the inner binary. For some system parameters, the pulsing Roche lobe can drive mass transfer at high rates. Systems undergoing this type of mass transfer include those with inner binaries consisting of compact objects that will eventually merge, as well as progenitors of Type Ia supernovae.

Key words: keyword1 – keyword2 – keyword3

1 ROCHE LOBE FOR A HIERARCHICAL TRIPLE

The concept of the Roche lobe is important to our understanding of binary evolution. When a star comes close to filling its Roche lobe its shape is distorted by tidal and rotational effects. When it fills its Roche lobe, it can transfer mass directly to its stellar companion through the L1 point. For higher order multiples, the simple Roche-lobe picture can serve only as an approximation [Di Stefano \(2018\)](#). Here we refine the picture in a way that is useful for the study of hierarchical triples.

We begin with the well-studied case of two stars with masses M_1 and M_2 in a circular orbit, with the spin frequency of Star 2 equal to the orbital frequency. We introduce the triple by replacing Star 1 by two stars, a and b with the same center of mass as M_1 and the same total mass: $M_a + M_b = M_1$. The orbital separation between a and b is small in comparison with the distance between their center of mass and Star 2. (See Figure 1.)

The L1 point of the original binary is that point lying between Star 1 and Star 2 at which the centripetal acceleration of a test mass is equal to the acceleration induced by the combined gravitational pulls of Star 1 and Star 2. The L1 point is therefore static in the corotating frame.

For a triple, there is generally no single frame within which all of the rotational frequencies are the same. In addition, the inner and outer orbits may occupy different planes. Because, however, we want to study cases in which Star 2 experiences tidal deformations and/or transfers mass, we will employ a “corotating frame”, coincident with the plane of

the outer orbit, in which Star 2’s spin frequency is equal to the frequency of the outer orbit. The L1 point is that point at which the centripetal acceleration of a test mass is equal to the acceleration induced by the combined gravitational pulls of Star a , Star b , and Star 2. Because Star a and Star b are moving, the location of this equilibrium point also moves.

In §2 we explore the motion of L1 points in hierarchical triples. We take the total mass of the system to be unity. Thus $M_1 + M_2 = 1$; $M_a = f M_1$, where f is a positive number less than unity, and $M_b = M_1 - M_a$. The distance between M_1 (which is at the center of mass of the inner binary) and M_2 is set to unity. The separation $2r$ between Star a and Star b must be significantly smaller than unity.

The energetics of mass moving within the binary system is described by an effective potential, $\Phi(r)$, which includes both gravitational and rotational effects. The L1 point connects two closed equipotential surfaces. Each of these equipotential surfaces encloses one of the two stars, forming that star’s Roche lobe. When Star 2 fills its Roche lobe, the L1 point is an escape hatch through which mass can start to travel toward Star 1.

The definition of the Roche lobes within a hierarchical triple is analogous to the binary-based definition. The difference is that the L1 point moves, and as it does, the value of the potential at the L1 point also generally changes. At any given instant, the Roche lobe of Star 2 is defined by the instantaneous value of Φ at the L1 point. As the value of Φ changes, so does the size and shape of the Roche lobe. These same statements apply to the Roche lobe that surrounds the inner binary.

* E-mail: rdistefano@cfa.harvard.edu

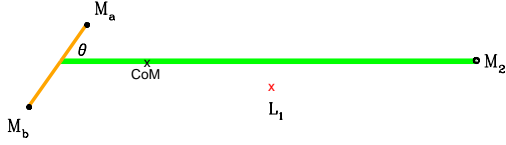


Figure 1. Hierarchical triple. Star 2 is connected by the thick green line to the center of the inner binary, whose axis is delineated by an orange (thinner) line. The three-body center of mass is marked “CoM”. If the pair M_a , M_b were replaced by a single mass $M_1 = M_a + M_b$, the L1 point would be located along the green line. The L1 point of the three-body system can, however, be located off the axis and it moves as the binary comprised of a and b rotates.

2 MOTION OF THE L1 POINT AND PULSATION OF THE ROCHE LOBE

2.1 Finding the L1 point

Star 2 is in a wide orbit with the inner binary, comprised of Stars a , b and 2 (Figure 1). The rotational period of Star 2 is the same as the period of the outer orbit. The total gravitational force on a test mass dm is

$$\vec{F}_{tot} = \vec{F}_a + \vec{F}_b + \vec{F}_2, \quad (1)$$

where \vec{F}_a , \vec{F}_b , and \vec{F}_2 are the gravitational forces exerted by Stars a , b , and 2, respectively. In order for the test mass dm to rotate with the outer binary, F_{tot} must be equal to the requisite centripetal force.

$$\vec{F}_{tot} = \vec{F}_{centripetal} \quad (2)$$

This condition defines the three-dimensional position of the L1 point (X_{L1}, Y_{L1}, Z_{L1}) . We take the point $(0, 0, 0)$ to be located at the CoM of the triple.

For the calculations we present here, the outer orbit lies in the $x - y$ plane, with Star 2 on the $+x$ -axis; the orbital angular momentum of the outer orbit is directed along the positive z -axis, which points outward toward the reader. Thus, in the co-rotating frame, the green axis (Figure 1) is fixed. The inner binary can rotate in any direction, with M_a and M_b traveling over the surface of three-dimensional spheres of radii r_a and r_b , respectively.

To create the descriptions and calculations presented in this paper, we have let the inner and outer orbital planes coincide. In this case: $x_a = r_a \cos(\theta)$, $y_a = r_a \sin(\theta)$, $x_b = r_b \cos(\theta + \pi)$, $y_b = r_b \sin(\theta + \pi)$. The z coordinates of all three masses are zero. By explicitly considering cases in which the inner and outer orbits are aligned, we derive results which can be easily described and which can also be readily generalized to systems in which the components of the inner binary move out of the plane of the outer orbit.

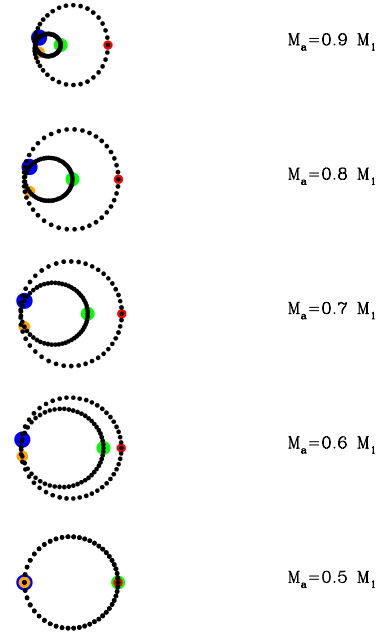


Figure 2. Curves followed by the L1 point. These triples each have $M_1 = 0.8$. They differ in the value of M_a , which varies from $0.9 M_1$ in the top panel to $0.5 M_1$ in the bottom panel. Each curve displays four special points corresponding to a value of the phase of the inner orbit: these points that get progressively larger and are colored differently, red ($\theta = 0$), orange ($\theta = \pi/2$), green ($\theta = \pi$), and blue ($\theta = (3\pi)/2$), in order of point size. The physical dimensions of the diameters of the largest circles shown above are 0.08 in units where the separation between star 2 and the center of mass of the inner binary is unity. As shown in §2.5, the size of the curves corresponding to those above would be smaller for smaller values of the inner-orbit separation.

2.2 Motion of the L1 point

The gravitational forces exerted on a test mass by Stars a and b change as the phase of the inner orbit changes. Thus, the point at which Equation (2) is satisfied, the L1 point, moves as the phase of the inner orbit changes. When Stars a and b lie along the x -axis, so that the three stars of the triple are aligned, the magnitude of the combined attractive force $\vec{F}_a + \vec{F}_b$ is generally larger than the magnitude of \vec{F}_1 , the force that would have been exerted by mass $M_1 = M_a + M_b$, located at the center of mass of the inner binary. Thus, to find a new point of equilibrium, the test mass must slide away from the inner binary and toward Star 2. Furthermore, unless $M_a = M_b$, the position of the L1 point is different at the inner binary phase $\theta = 0$ (when the more massive star, Star a , is closer to Star 2), from its position at phase $\theta = \pi$ (when the less-massive star, Star b , is closer to Star 2). At phase $\theta = \pi/2$, the magnitude of the combined force $\vec{F}_a + \vec{F}_b$

is smaller than for $\theta = 0$, or $\theta = \pi$ ¹. The L1 point therefore moves *toward* the inner binary and *away from* Star 2. For other inner-binary phases, both Stars *a* and *b* lie off the x -axis, and the L1 point must also move off of the x -axis.

Figure 2 illustrates the motion of the L1 point in five different triple-star systems. For each triple in Figure 2, $M_1 = M_a + M_b = 0.8$ and $M_2 = 0.2$. The difference among the triples is in the value of f : $M_a = f M_1$, as labeled. First we consider a single curve. Each point on the curve corresponds to the position of the L1 point at a specific phase of the inner orbit. For the purpose of focusing on the magnitude of the changes, the origin of the coordinate system for each of the five triples shown was chosen to be the symmetry point. In each curve, the point in red (smallest of the 4 specially marked points) corresponds to $\theta = 0$. This is the phase at which the combined gravitational pull exerted by Stars *a* and *b* is at its maximum. Hence, the L1 point is farthest from the center of mass of the inner binary and is closest to Star 2. The point in orange (next largest) corresponds to $\theta = \pi/2$. Proceeding to larger points, green is for $\theta = \pi$ and blue is for $\theta = (3\pi)/2$. The point in green ($\theta = \pi$) is where all three masses are aligned, and Star *b* ($M_b < M_a$) closest to M_2 .

Moving downward from the top curve: as the value of f approaches $1/2$, the green point moves progressively closer to the red point ($\theta = 0$). As long as the values of M_a and M_b are different, points for $\theta = \pi/2, ((3\pi)/2)$, lie slightly below (above) the x -axis, to allow M_2 to counter the net upward (downward) gravitational tug of the inner binary. The L1 point executes a closed curve which, except for the case in which $M_a = M_b$, self intersects. On each curve, the time between neighboring black points is $2\pi/100$. Thus, larger spatial distances between adjacent black points show places where the speed of the L1 point was larger,

In Figure 2, the diameter of the largest circular curve is 0.08 of the distance between Star 2 and the center of mass of the inner binary. These dimensions are tied to the separation between the stars in the inner orbit. We will explicitly discuss this point in §2.5.

In general, the details of the motion of the L1 point depend on the relative orientations of the two orbits, and on whether the orbits are eccentric. Depending on the relative orientation of the planes of the inner and outer orbits, the motion of the L1 point can be three dimensional. The considerations above, of how the combined gravitational force of the two components of the inner binary influences the position of the equilibrium point, are generally valid and provide a way to extend the results to a wide range of hierarchical triples.

2.3 Dependence on M_1/M_2

To systematically explore the effect of varying the mass ratio M_1/M_2 , we considered two sets of hierarchical triples. In the first set (top panel of Figure 3) the masses of the inner binary were equal ($M_a = M_b$). In the second set (bottom panel), $M_a = 0.8 M_1$, so that $M_a = 4 M_b$. To create the curves in each panel, we varied the value of M_1 and M_2 , with the sum $M_1 + M_2$ always equal to unity. The smallest value of M_1 we

considered was 0.01, which would generally correspond to a case in which the inner binary consists of orbiting brown dwarfs or planets. The largest value was 0.99.

To create both the top and bottom panels we first computed the position $x(L1, 2)$ of the L1 point for a binary with $M_2 = 1 - M_1$. The L1 point lies along the x -axis. We then considered configurations of the inner binary for which the L1 point of the hierarchical triple also lies along the x -axis.

In the top panel of Figure 3, where the masses of the components of the inner binary are equal, there are two such configurations. In the first (shown in red; topmost curves), Stars *a* and *b* both lie along the x -axis. In the second configuration (shown in brown; bottommost curves), Stars *a* and *b* both lie along the y -axis.

For each configuration of the inner masses, we considered the full range of values of M_1 described above. For each value of M_1 we computed the location $x(L1, 3)$ of the L1 point in the corresponding hierarchical triple. In Figure 3, the difference $x(L1, 3) - x(L1, 2)$ is plotted against M_1 . The solid curves correspond to inner binaries in which the inner-binary separation, R_{in} is roughly 0.2 (see §2.5). For the dotted curves, R_{in} is only half as large.

The curves shown in the bottom panel of Figure 3 are analogous, but with $M_a = 0.8 M_1$. The inner-binary configurations for which the L1 point of the hierarchical triple lies along the x -axis are those in which Stars *a* and *b* are colinear with Star 2. There are two independent configurations with this geometry: (1) M_b , the smaller mass, is closer to Star 2; (2) M_a is closer to Star 2.

The top and bottom panels combine to tell a unified story. When the three masses are co-aligned, the L1 point moves out, toward Star 2. When the two masses lie along the perpendicular direction (i.e., the axis proceeding from the inner-binary CoM to M_2 is perpendicular to the axis proceeding from M_b to M_a), the L1 point is pulled back toward the inner binary. The magnitude of the change is sensitive to the separation of the inner binary.

We also note that, in the range of M_1 values over which both M_1 and M_2 contribute significantly to the mass budget, the change in L1 depends only slightly on the value of M_1 , edging up gradually as M_1 increases. At larger values (with M_1 larger than $\sim 0.85 - 0.9$), where Star 2 could be a brown dwarf or planet, the motion of the L1 point significantly increases in magnitude as M_1 increases.

2.4 Pulsation of the Roche Lobe

When the L1 point moves in toward Star 2, it is moving to places where the magnitude, $|\Phi|$, of the gravitational-rotational potential is larger. The corresponding equipotential surface, the Roche lobe, is therefore generally *smaller*. On the other hand when the L1 point moves away from Star 2, the potential defining the Roche lobe has a smaller absolute magnitude and the Roche lobe is therefore larger. The result is that the Roche lobe pulsates as the inner orbit proceeds.

Figure 4 illustrates this effect. In both top and bottom panels, the golden curve shows the Roche lobe of a binary with $M_1 = 0.8$ and $M_2 = 0.2$. The top panel corresponds to the case in which $M_a = M_b$. The inner-orbital phase is $\theta = 0$, (equivalent in this case to $\theta = \pi$) for the Roche lobe shown in red. As predicted in the discussion above, the L1 point has

¹ It is also smaller than it would have been for M_1 alone.

moved toward Star 2, i.e., toward larger values of $|\Phi|$, and the Roche lobe surrounding Star 2 is smaller than Star 2's binary-only Roche lobe. The Roche lobe surrounding the inner binary is stretched along the horizontal direction. In brown is the Roche lobe for $\theta = \pi/2$, for which the lobe surrounding Star 2 is larger, and the lobe surrounding the inner binary is stretched along the vertical direction. In both the top and bottom panels, the values of R_{in} are roughly equal to 0.2 (§2.5).

In the bottom panel of Figure 4, $M_a = 0.8 M_1$, and $M_b = 0.2 M_1$. The curve in blue corresponds to $\theta = 0$, in which Star *a* is closer to Star 2 than is Star *b*. In purple is the Roche lobe for $\theta = \pi$. In both phases, the total gravitational force exerted by Stars *a* and *b* exceeds the force that would be exerted by M_1 , so that both Roche lobes surrounding Star 2 are smaller than for the pure binary case.

2.5 The Size of the Inner Binary

The magnitude of the motion of the L1 point depends on the size of the inner binary relative to the separation of the third star from the center of mass of the inner binary. If the inner binary is too wide, the triple is not hierarchical, and it also may not be dynamically stable.

Conditions for dynamical stability have been derived and also compared with data for hierarchical triples composed of point masses (Eggleton & Kiseleva 1995; Mardling & Aarseth 2001; Tokovinin 2018b). The smallest ratio of orbital periods between the closest orbits in observed hierarchical triples is typically ~ 5 , corresponding to a ratio in orbital separations of ~ 0.3 . In the examples considered here, the largest ratio we considered was used $R_{in} \approx 0.2$.² The stability conditions may be less restrictive when the donor star is filling its Roche lobe, because tidal forces are also important, and may enhance stability. In addition, once mass from the donor begins to interact with the inner binary, this interaction may play the key role in determining the fate of the inner binary, at least until the pool of mass from the donor is exhausted.

The L1-point motions depicted in Figure 2 and in the solid curves of 3 were generated by inner binaries with $R_{in} = 0.17$ for the equal-mass inner binary, and $R_{in} = 0.23$ for the inner binary with $M_a = 0.8 M_1$. The dotted curves in Figure 3 reveal that there is a significant dependence on the on R_{in} , the radius of the inner binary. The dependence is explored in more detail in Figure 5, where we varied the value of R_{in} . Here we considered the

To create Figure 5 we again considered the hierarchical triples with $M_1 = 0.8$. For both an equal-mass inner binary (solid lines), and one with $M_a = 0.8 M_1$ (dashed lines), we varied the value of R_{in} , the radius of the inner orbit, and recorded the values of the x -coordinate and y -coordinate of the L1 point and also the radius of the Roche lobe. To quantify the change in Roche lobe radius, we defined Δ_{RL} to be the different between the largest and smallest value of R_L achieved during a complete cycle of the inner orbit. Similarly, Δ_x (Δ_y) is the difference between the largest and

smallest value of x (y) achieved during one cycle of the inner orbit. The figure shows how the value of each Δ depends on the value of R_{in} . For $R_{in} \approx 0.25$ the change in Roche lobe radius over the course of one inner orbit is roughly 5%, and the slope of the log-log plot is roughly equal to -2 .

3 IMPLICATIONS

3.1 The Dynamical Roche Lobe and New Modes of Mass Transfer

The donor star in a simple binary comes to fill its Roche lobe because the Roche lobe shrinks and/or the donor expands. To simplify the discussion below we will discuss the case in which the Roche lobe shrinks because the separation between the donor and accretor is decreasing due to the loss of orbital angular momentum associated with, for example, magnetic braking. Text describing Roche-lobe filling due to increasing stellar size would be directly analogous. When the Roche lobe shrinks to the size of the donor star, the donor can send mass through the L1 point to its companion. The initiation of mass transfer influences both the orbital separation and the size of the donor star. As long as the relative sizes of the Roche lobe and donor star continue to be well matched, mass transfer is stable.

Shifting our consideration to the case in which the accretor is a binary, we continue to focus on donor-to-accretor mass ratios where stable mass transfer would occur, were the accretor a single star. Because the accretor is a binary, the Roche lobe is not only shrinking, but is also pulsating. Prior to mass transfer, the donor fits within the smallest Roche lobe associated with the inner binary.

As time goes on, the average volume of the Roche lobe continues to shrink. During some portions of the inner orbit, the Roche lobe will touch the donor's surface, and then withdraw. The relatively small amount of mass lost during the brief intervals of Roche-lobe filling may not be enough to allow the system to come into equilibrium. Thus, over times longer than the inner orbital period, the size of the Roche lobe may continue to shrink. When this happens, the star will overflow the smallest Roche lobe part of the time, but may not fill the maximum-radius Roche lobe produced by the inner orbit. The pulsations of the Roche lobe would therefore introduce a periodicity to the mass flow. Preliminary hydrodynamic simulations find that mass loss is enhanced with a periodicity equal to that of the inner binary.

$$\dot{M}_{dyn} = -\kappa \frac{M_2}{P_{out}} \left(\frac{R_2 - R_{RL}}{R_2} \right)^{n+\frac{3}{2}}, \quad (3)$$

where n is the polytropic index of Star 2, P_{out} is the orbit period of the outer orbit, and κ is a number whose value is typically of order unity. [See MacLeod et al. (2018) and references therein.]

It is useful to consider some specific examples. Let's represent $(R_2 - R_{RL})/R_2$ by 0.01β . We can consider a binary with $M_1 = 8 M_\odot$ and take Star 2, with mass $M_2 = 2 M_\odot$, to be filling its Roche lobe. In our first example, we allow Star 2 to be evolved, with $n = 3/2$ and a radius of $50 R_\odot$.

² In the units we employed, with the size of the outer orbit set equal to unity, R_{in} is the ratio between the radii of the inner and outer orbits.

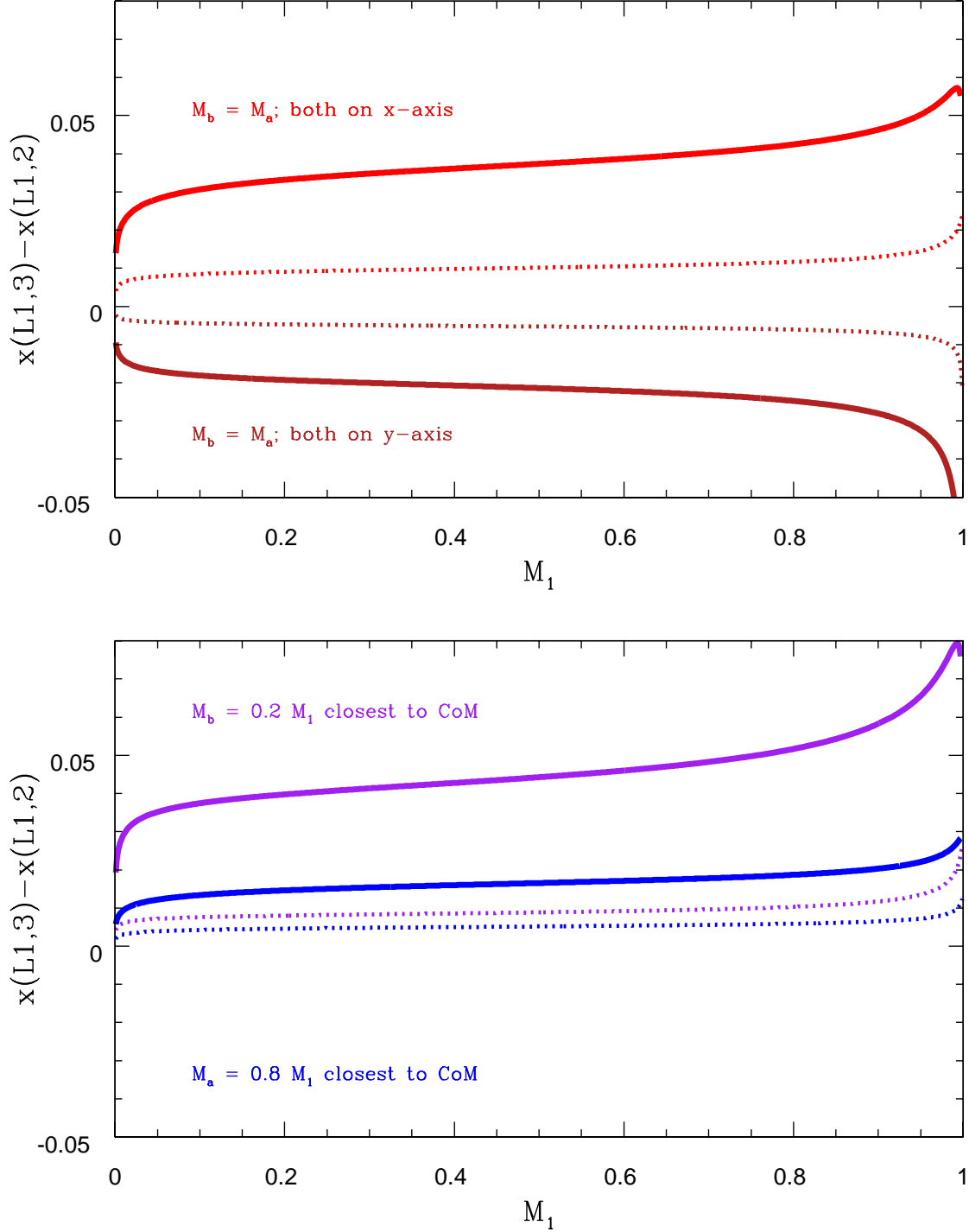


Figure 3. Positions of the L1 point for hierarchical triples, as a function of the binary mass, $M_1 = M_a + M_b$. *Top panel:* $M_a = M_b = 0.5 M_1$. Solid curves: $R_{in} = 0.17$; dashed curves: $R_{in} = 0.085$. Curves in red (top two curves) correspond to both a and b being on the x -axis. Curves in brown (bottom two curves) correspond to both a and b being on the y -axis. *Bottom panel:* $M_a = 0.8 M_1$; Star a and Star b are both on the x -axis. Solid curves: $R_{in} = 0.23$; dashed curves: $R_{in} = 0.115$. Curves in blue (bottom solid curve and bottom dotted curve) correspond to the situation in which M_a is closer to Star 2. In purple are the curves corresponding to the case in which M_b is closer to Star 2.

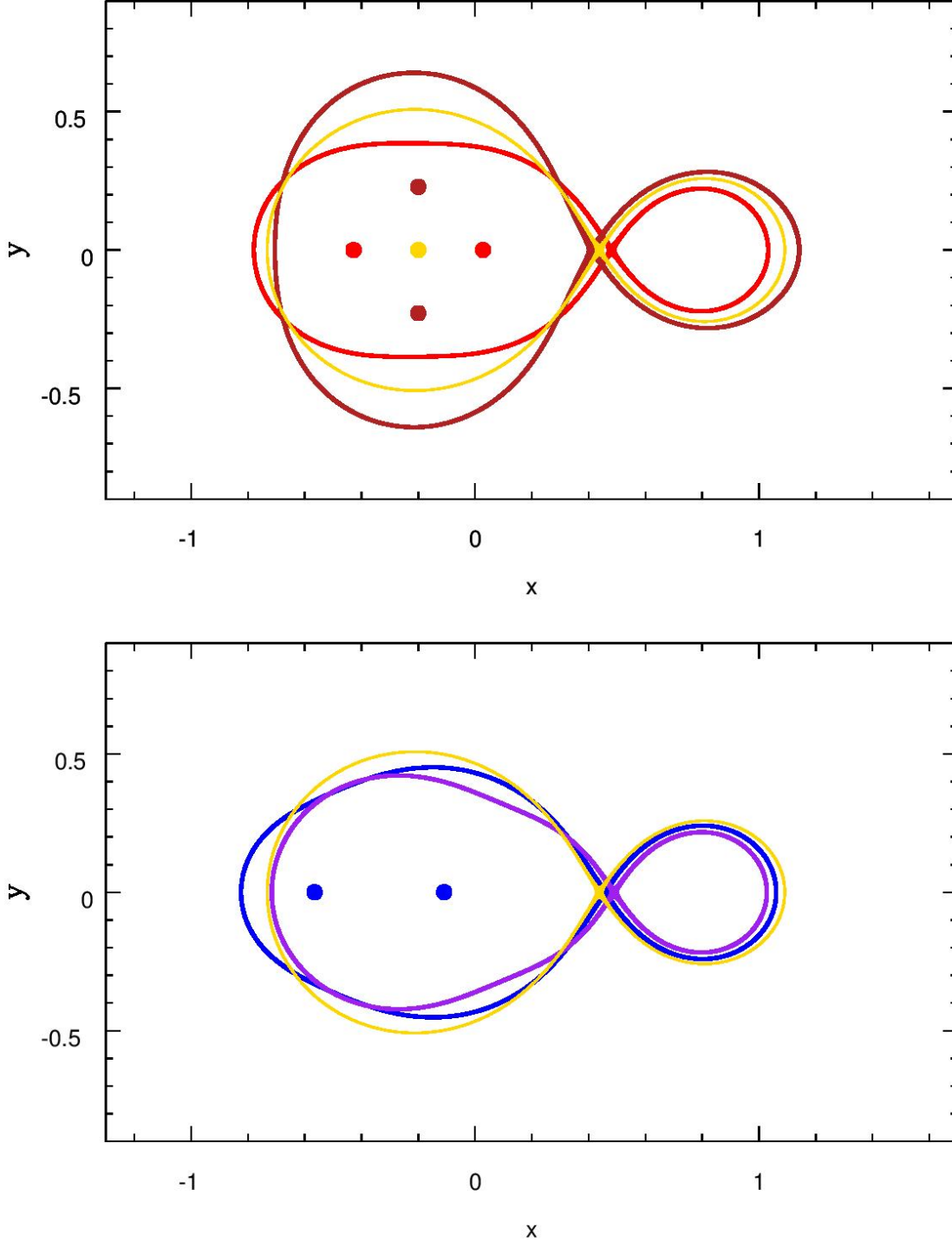


Figure 4. Shapes of the Roche lobes for hierarchical triples. In all cases shown, $M_1 = 0.8$. *Top:* $M_a = M_b = 0.5 M_1$; $R_{in} = 0.17$. The red curve (which is elongated along the x -axis on the left) corresponds to both a and b being on the x -axis (red points). The brown curve (which is elongated along the y -axis on the right) corresponds to both a and b being on the y -axis (brown points). Here and also in the bottom panel, the inner binary (a - b) has been replaced by a point mass to produce the curve in gold. *Bottom:* $M_a = 0.8 M_1$; $R_{in} = 0.2$; Star a and Star b are both on the x -axis. Curves and points in blue (purple) correspond to the situation in which M_a (M_b) is closer to Star 2. The blue dots mark the inner-star positions for the blue curve. The positions for the purple curve are not included, simply to avoid confusion.

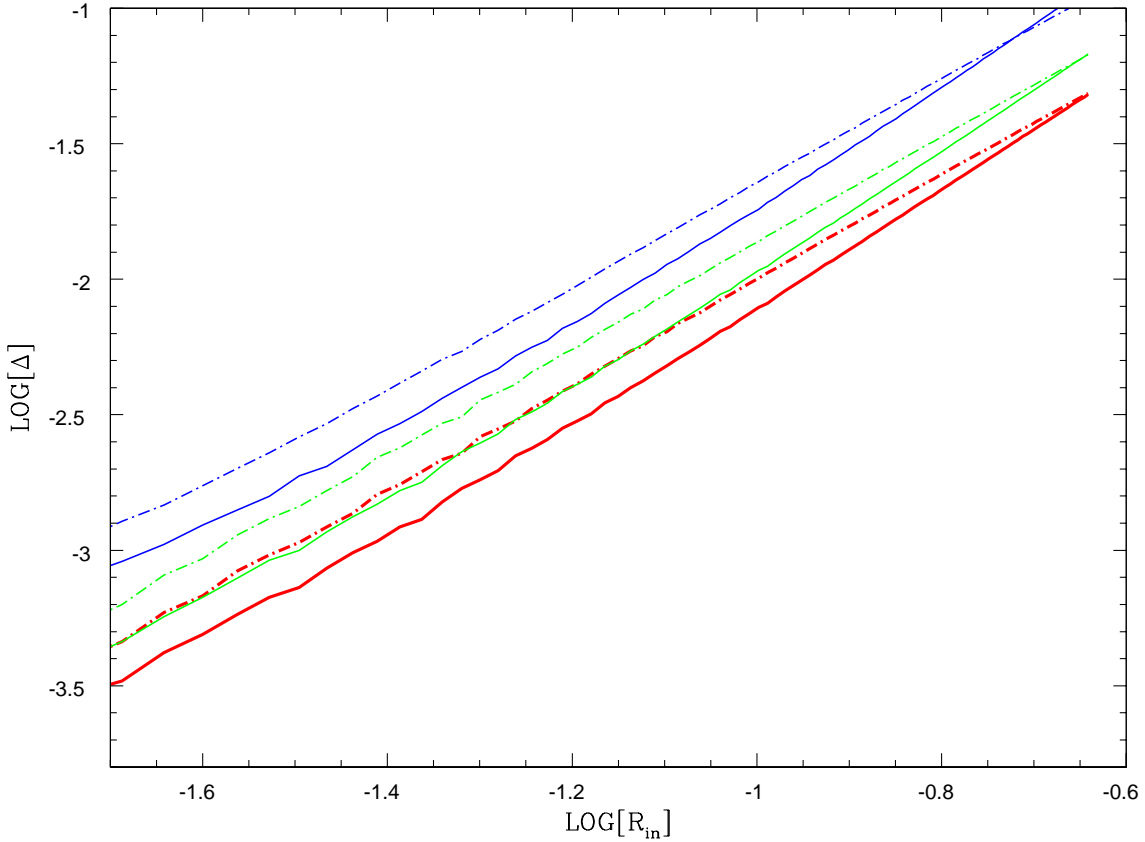


Figure 5. The logarithm to the base ten of the absolute magnitude of the change in size (Δ) versus the logarithm to the base ten of R_{in} . In red, the change in size refers to the difference between the maximum and minimum radii achieved by the Roche lobe during the course of a complete orbit of the inner binary. In green (blue) the change in size refers to the absolute magnitude of the maximum difference between the x -coordinate (y -coordinate) of the L1 point. In all cases shown here $M_1 = 0.8$. Dashed lines (solid lines) are for hierarchical triples with $M_a = M_b$ ($M_a = 4 M_b$).

In this case, the orbital period is roughly 94 days and

$$\dot{M}_{dyn} = -\kappa \beta^3 \left(7.8 \times 10^{-6} \right) \frac{M_{\odot}}{\text{yr}}, \quad (4)$$

To consider a $2 M_{\odot}$ main-sequence donor, we take $n = 3$. The outer binary has an orbital period of 0.76 days and

$$\dot{M}_{dyn} = -\kappa \beta^{4.5} \left(1 \times 10^{-6} \right) \frac{M_{\odot}}{\text{yr}}. \quad (5)$$

3.2 Systems with High \dot{M}_{dyn}

Equations (4) and (5) show that pulsations of the Roche lobe have the potential to produce high values of the mass transfer rate. In the case of a hierarchical triple with mass transferred from the outer star, high rates of accretion produce high X-ray luminosities if one or both of the components of the inner binary are compact objects.

When matter is accreting onto a neutron star (NS) or black hole (BH), perhaps $0.1 \dot{M} c^2$ can be emitted in the

form of radiation. For $\dot{M}_{dyn} = 10^{-6} M_{\odot} \text{ yr}^{-1}$, the associated luminosity is $5.7 \times 10^{39} \text{ erg s}^{-1}$, corresponding to an ultraluminous X-ray sources (ULX). (See Israel et al. (2017) and references therein.) ULXs are rare, with some galaxies having none, while galaxies with high rates of star formation may have more than one. [See Bachetti et al. (2013); Dage et al. (2019) and references therein.] If, therefore, hierarchical mass-transfer binaries contribute even one such system per (1-10) galaxies, their contribution would be significant.

For white-dwarf (WD) accretors, rates of infall in the ranges consistent with equations (4) and (5) would produce quasisteady nuclear burning Iben (1982); Nomoto (1982); Shen & Bildsten (2007). The resulting luminosities would be a few times $10^{38} \text{ erg s}^{-1}$. It is not clear what fraction of such systems emit at X-ray wavelengths Di Stefano (2010b,a), although their bolometric luminosities would be large. Nuclear burning on the surface of a WD can allow infalling mass to be retained, resulting in a Type Ia supernova through the so-called *single degenerate* channel, Rappaport et al. (1994) or else an accretion-induced collapse van den Heuvel et al. (1992).

Note that \dot{M}_{dyn} is associated with the pulsation of the Roche lobe. If the accretor were a single mass (rather than a binary), Roche-lobe filling by the same donor star would produce mass transfer at some rate \dot{M}_0 . The value of \dot{M}_0 is determined by the state of evolution of the donor (e.g., is it expanding? is it emitting winds?) and on the influence of any dissipative forces that drive the donor and accretor closer to each other. Thus, the total mass transfer rate is

$$\dot{M} = \alpha \dot{M}_0 + \beta \dot{M}_{dyn}, \quad (6)$$

where α and β are each constants with values between 0 and 1.

Mass transfer to the inner binary can increase the masses of its components. It can also drive Stars *a* and *b* closer to each other (Di Stefano (2018)). Thus, the two stars in the inner binary can each gain mass. At the same time, the pair is more likely to merge sooner. This has implications for both the rates of gravitational mergers and for the rates of WD-WD mergers, some of which may produce Type Ia supernovae through the *double-degenerate* channel.

Whether the components of the inner binary are low-mass objects, stars, or compact objects, the decrease of the separation between Stars *a* and *b* will decrease the value of \dot{M}_{dyn} , the magnitude of the Roche lobe's pulsations, and also the size of the L1 point's excursions. The system will act more like an ordinary binary and, if the inner stars merge, it will in fact become a binary.

3.3 Accretion Flow

When the accretor is a binary, the L1 point moves around a small region of the donor star. Mass is released from a sequence of different places with different velocities. Thus, the distances, speeds, and angles of approach to the accretor's center of mass differ from what they would have been in a simple binary. Not only is the mass sent from different launch points, but the potential is also changing. The larger the inner binary, the larger the magnitude of variations in the potential, even in the region that would, for an isolated binary, be occupied by the outer disk. This may make it impossible for a circumbinary disk to form. Accretion within the largest inner binaries may therefore proceed through separate accretion by each of its stars.

For smaller inner binaries, however, circumbinary disks may be expected. In the case of supermassive BHs, "mini-disks" can then form around the individual components of the close binary [e.g., Bowen et al. (2017)]. When conditions are analogous for stellar mass binaries, the same should happen. Indeed, preliminary hydrodynamic studies Shroder et al. (2019) find that the regions around the inner stars accumulate matter at relatively high densities. This discussion indicates that the accretion flows in hierarchical triples are likely to exhibit a variety behaviors and will require careful study.

Apart from the intrinsic interest of the problem, it is important to understand how much mass can be accreted by each component of the inner binary and how much mass is ejected. The amount of angular momentum carried away by mass ejected from the vicinity of the inner binary plays an important role in determining the future of the binary.

3.4 Do Hierarchical Triples With Mass Transfer Exist?

It is important to demonstrate that there are three-body systems in which a close binary can come to receive mass from a star in a wider orbit. In such systems, the size of the donor determines the size of the Roche lobe: $R_L = R_2$. This, together with the mass ratio, $q = M_2/M_1$, sets the size of the outer orbit.

$$a_{out} = \frac{R_2}{f(q)}, \quad (7)$$

where $f(q) = 0.49 q^{\frac{2}{3}} / (0.6 q^{\frac{2}{3}} + \ln(1 + q^{\frac{1}{3}}))$ (Eggleton 1983).

In addition to the Roche-lobe filling condition above, the system must satisfy conditions for orbital stability. Such conditions have been derived for hierarchical triples in which the components have constant mass Eggleton & Kiseleva (1995); Mardling & Aarseth (2001). When a star that fills or is close to filling its Roche lobe donates mass, the conditions will be different, as both energy and angular momentum are associated with tides and with mass flowing through and from the system. Here we use the simplest form of the condition required for orbital stability of the hierarchical triple, expressed in terms of a ratio of the outer to inner orbital periods, $P_{out}/P_{in} > \eta$, where $\eta = 5\eta_0$, where $\eta_0 \approx 1$ Mardling & Aarseth (2001); Tokovinin (2018a). When tides and/or mass flow serve to stabilize the orbits, the effective value of η_0 is smaller.

Dynamical stability puts an upper limit on the size of the inner binary for a given value of a_{out} .

$$a_{in} = a_{out} \left[\frac{M_{in}}{M_T} \left(\frac{P_{in}}{P_{out}} \right)^2 \right]^{\frac{1}{3}} < \left(\frac{0.34}{\eta_0^{\frac{2}{3}}} \right) \left(\frac{R_2}{f(q)} \right) \left(\frac{M_{in}}{M_T} \right)^{\frac{1}{3}} \quad (8)$$

To provide perspective, we note that $f(0.1) = 0.21$, and $f(0.9) = 0.37$. Thus, the separation between the components of the inner binary can at largest be comparable to the radius of the outer Roche-lobe-filling star.

The condition for orbital stability must be supplemented by the condition that mass transfer be stable. Stability of mass transfer generally requires that the donor be less massive than the accretor or that, if it is more massive, it is able to shrink when it loses mass. Putting these conditions together provides a lower bound on the total mass of the inner binary relative to the mass of the main-sequence donor. At the same time, there is an upper bound on the size of the inner binary. Fortunately, a wide range of hierarchical triples satisfy these conditions.

3.4.1 Main-Sequence Donors

Given the conditions sketched above, it is clear that when the donor is on the main sequence, a_{in} is generally smaller than a few solar radii. Stars *a* and *b* must therefore fit within a small orbit. One possibility is that both Stars *a* and *b* can be stellar remnants. If the masses of one or both remnants are comparable to or larger than a solar mass, a gravitational merger will occur with a Hubble time. Mass donated by the outer star can increase their masses, and shorten the time to merger. In addition, mass transfer may continue through the

time of merger, becoming a source of electromagnetic radiation prior to and during merger. Post merger, mass transfer onto the merged object may continue. [See [Di Stefano \(2018\)](#) for details.] When the donor is a main-sequence star and the inner binary is composed of stellar remnants, the question of how the triple evolved to its present state arise. This scenario seems most likely in dense clusters. Note that, in addition to compact-object inner binaries, there are other possibilities. For example, the inner binary could contain one or two low-mass stars and/or brown dwarfs.

3.4.2 Subgiant or Giant Donors

When the donor is a giant or subgiant, its radius, hence the largest allowed size of the inner orbit, is larger. This means that inner binaries with larger donor stars can be accommodated. All of the binary types allowed for main-sequence donors are still possible. But now Stars *a* and *b* may both be main-sequence stars of larger mass and therefore with larger radii. The case in which the inner binary consists of main sequence stars is intriguing, because the hierarchical triple could then have a primordial origin, like many of the higher-order multiples being discovered in ongoing surveys.

3.5 Conclusion

Mass transfer within hierarchical triples may have interesting consequences, and has only begun to be systematically explored ([Di Stefano 2018](#)). While detailed simulations will play important roles in elucidating the behavior of such systems, here we have used the concept of the L1 point and Roche lobe to predict and explain key features. In particular, over a wide range of ratios of the inner to outer semi-major axes, mass transfer will be imprinted with the time signature of the inner orbital period. Furthermore, for large values of this ratio, the pulsation of the Roche lobe may drive mass transfer at high rates. Mass transfer hierarchical triples with NS and/or BH accretors may reach the luminosities (above $10^{39} \text{erg s}^{-1}$) associated with ULXs. When the accretor is a WD dwarf, the rates may be high enough to promote genuine mass gain by the WD dwarf.

The investigation described here is theoretical, and the results indicate that if hierarchical triples are not rare, they may already have been observed as systems of high astrophysical interest.

REFERENCES

- Bachetti M., et al., 2013, [ApJ](#), 778, 163
 Bowen D. B., Campanelli M., Krolik J. H., Mewes V., Noble S. C., 2017, [ApJ](#), 838, 42
 Dage K. C., Zepf S. E., Peacock M. B., Bahramian A., Noroozi O., Kundu A., Maccarone T. J., 2019, [MNRAS](#), 485, 1694
 Di Stefano R., 2010a, [ApJ](#), 712, 728
 Di Stefano R., 2010b, [ApJ](#), 719, 474
 Di Stefano R., 2018, arXiv e-prints
 Eggleton P. P., 1983, [ApJ](#), 268, 368
 Eggleton P., Kiseleva L., 1995, [ApJ](#), 455, 640
 Iben Jr. I., 1982, [ApJ](#), 259, 244
 Israel G. L., et al., 2017, [Science](#), 355, 817
 MacLeod M., Ostriker E. C., Stone J. M., 2018, [ApJ](#), 863, 5
 Mardling R. A., Aarseth S. J., 2001, [MNRAS](#), 321, 398
 Nomoto K., 1982, [ApJ](#), 253, 798
 Rappaport S., Di Stefano R., Smith J. D., 1994, [ApJ](#), 426, 692
 Shen K. J., Bildsten L., 2007, [ApJ](#), 660, 1444
 Shröder S., MacLeod M., Di Stefano R., Knight A. H., 2019
 Tokovinin A., 2018a, [AJ](#), 155, 160
 Tokovinin A., 2018b, [ApJS](#), 235, 6
 van den Heuvel E. P. J., Bhattacharya D., Nomoto K., Rappaport S. A., 1992, [A&A](#), 262, 97